Nano World Journal

https://doi.org/10.17756/nwj.2023-s5-003

Review Article

Open Access

Investigation of Sintering Temperature Effect on the Sol-gel Synthesized Titanium Dioxide Nanoparticles and Dielectric Constant Determination Using Impedance Spectroscopy

Inbanathan Flavia Princess Nesamani[1], M. Manikandan[2], M. Kalpana[3], Aswathy Paul[3] and Dhivyasri Gopal[4*]

[1]*EET, CATS, Kent State University at Trumbull, USA*
[2]*Department of Electronics and Communications Engineering, School of Engineering, Presidency University, Karnataka, India*
[3]*Karunya Institute of Technology and Sciences, Coimbatore, Tamil Nadu, India*
[4]*Sai Vidya Institute of Technology, Karnataka, India*

***Correspondence to:**
Dhivyasri Gopal
Sai Vidya Institute of Technology,
Karnataka, India.
E-mail: dhivyaasrigopal@gmail.com

Received: October 11, 2023
Accepted: December 18, 2023
Published: December 21, 2023

Citation: Nesamani IFP, Manikandan M, Kalpana M, Paul A, Gopal D. 2023. Investigation of Sintering Temperature Effect on the Sol-gel Synthesized Titanium Dioxide Nanoparticles and Dielectric Constant Determination Using Impedance Spectroscopy. *NanoWorld J* 9(S5): 14-17.

Copyright: © 2023 Nesamani et al. This is an Open Access article distributed under the terms of the Creative Commons Attribution 4.0 International License (CCBY) (http://creativecommons.org/licenses/by/4.0/) which permits commercial use, including reproduction, adaptation, and distribution of the article provided the original author and source are credited.

Published by United Scientific Group

Abstract

The nanoparticles of titanium dioxide (TiO_2) are experimentally formed by sol-gel process with titanium isopropoxide as a precursor along with ethanol and distilled water. Nitric acid is mixed to change the value of pH in the solution. Thus, synthesized titania (TiO_2) in the gel form is of amorphous phase with a particle size ranging from 2 nm to 5 nm at a sintering temperature of 450 °C and then gets transformed into an anatase phase with a crystallite size ranging from 9.78 nm to 15.75 nm for sintering temperature above 450 °C. The functional group identification, crystal size, structural and morphological studies are done by FTIR (Fourier transform infrared) spectroscopy, XRD (X-ray diffraction), TEM (Transmission electron microscope), and SEM (Scanning electron microscope), respectively.

Keywords

Nanoparticles, Synthesis, Titania, Characterization

Introduction

TiO_2 nanomaterials are found to be of substantial usage potential in a wide range of industries, including pollution reduction, ceramic, cosmetic solar cells, and analytical components [1]. TiO_2's non-toxicity, simplicity of handling, and low cost of production are its main draws. Despite a variety of synthesis techniques, the solvothermal process and solgel process remains the easy methods for creating TiO_2 nanoparticles with the desired physical and optical property. The solvothermal process can produce nanoparticles, nanorods, nanotubes, and other types of nanostructures that are excellent for creating nanomaterials. The reaction time, temperature solvent type, and autoclave pressure are process variables to achieve these kinds of nanostructures. Additionally, the solution pH, aging time and chemical composition can all be adjusted to affect particle morphology and crystallinity. Compared to other chemical approaches, this method yields fine particles with distinctive physical properties.

Due to lower pressure and temperature, the sol-gel method is similar to solvothermal synthesis but simple. This method gives you the freedom to adjust the compositional and microstructural characteristics of the nanoparticles depending on the synthesis conditions and characteristics. Since precipitates produced by the solgel process are amorphous in nature, the crystallinity of the sample must be achieved through calcination at an appropriate temperature. Furthermore, because of the expansion of the grain boundaries, calcination at a higher temperature and aggregation of the particles may encourage phase transformations [2].

TiO_2 has been extensively studied and analyzed as the gate dielectric in MOSFETs [3-12], photocatalysis [13, 14], solar energy conversion [15-17], and

electrochemical capacitors [18]. For the synthesis of TiO_2 nanoparticles, various chemical methods are used that includes the sol-gel method [19-23], hydrothermal synthesis [24-26], reversed micelle method [27-28], cathodic electrodeposition [29], chemical vapor deposition [30], reactive sputtering [31, 32]. From the numerous syntheses, the sol-gel technique is considered as a promising and most successful technique for preparing nanocrystalline metal oxide materials as it offers the significance of macro-porous coating done at a low cost and also a relatively easy process control [33-38]. In this work, TiO_2 is synthesized using sol-gel method to yield amorphous TiO_2 which is similar to amorphous SiO_2 with much reduction in the leakage current of a MOSFET, upon sintering, a phase transition to anatase phase is observed. Although the electronic bandgap of this material is (3.5 eV), it is considerably small, and its dielectric constant can be varied from 88 to 110.

Experimentation

Synthesis

TiO_2 can be synthesized either from the precursor titanium(IV) chloride and titanium alkyl oxide. In this work, TiO_2 is synthesized in a round bottom glass flask, and under vigorous stirring, 10 ml of titanium isopropoxide is added drop by drop to the mixture of 10 ml of distilled water and 30 ml of absolute ethanol. The stirring process continues for 1 h. The pH value is found to be between 4 and 5. Then 0.1 N nitric acid is added to avoid the agglomeration process and control the pH as well until TiO_2 particle synthesis is completed. The solution is then vigorously stirred to form sols. After 24 h, the sols are transformed into gels to obtain the nanoparticles. The gels are dried under 1200 °C for 2 h to evaporate organic material and water to a maximum extent. Then the dried gel is sintered at 4500 °C for 2 h subsequently to obtain desired nanoparticle TiO_2. Then the sample is once again sintered up to 750 °C to monitor the stability of the sample.

Characterization

The absorption spectrum of the TiO_2 samples is obtained using SCHIMADZU IR Prestige-21 with 410 - 4000 cm^{-1} wavelength range and resolution of 2 cm^{-1} using KBr pelletizer. A CuK target with a voltage of 40 kV, a sample pitch of 1, and a scan mode are used to achieve the X-ray diffraction in the Schimadzu, XRD 6000 (Japan Model) at room temperature. The scan moves at a 10°/min speed. SEM analysis is carried out using a JEOL microscope of model JSM-6390. For SEM measurement, the samples are combined with ethanol, ultrasonically blasted, and set on a carbon film strengthened on a grid made up of copper.

The TEM investigation is made using JOEL JM 2010. The structural, chemical, and morphological information is analyzed with high resolutions. The samples are subjected to electron diffraction crystallographic analysis and a selected area electron diffraction pattern was obtained. For the TiO_2 sample, convergent beam electron diffraction patterns are also obtained. TiO_2 and ethanol are blended, ultrasonically processed for five minutes, and then placed on a copper grid covered in carbon. For the impedance analysis, the powder is sprayed onto a die with a 10 mm diameter and a 1.29 mm thickness while being applied with 200 psi of pressure. The powder is then given a 5-min pause before being used to generate patterns. The pellet is sintered at 450 °C for an hour before being calcined at various temperatures up to 750 °C.

The impedance measurement is done using Impedance Analyzer Hioki 3532-50 LCR Hi TESTER varying frequency range from 42 Hz - 5 MHz at room temperature and higher temperatures from 50 °C to 400 °C at intervals of 50 °C. The electrodes are not applied on the substrate to avoid diffusion effects. The sample is certain to come into contact with the pressure contact electrodes, though.

Results and Discussion

The XRD patterns of amorphous and crystalline anatase phase TiO_2 are shown in figure 1. The amorphous phase of TiO_2 can be transformed into a crystalline phase of TiO_2 using two approaches. One by adding nitric acid momentarily and another by sintering and both approaches are used in this synthesis method. The pH observed is 7 after adding nitric acid and the sintering process with temperatures up to 450 °C resulted in an amorphous phase with clusters of particles with size ranging from 2.19 nm to 5.298 nm, but with more agglomeration, as shown in figure 1a. For sintering temperatures above 450 °C, the synthesized TiO_2 had a transition from amorphous to anatase phase with a particle size of 80 nm to 130 nm and a crystallite size ranging from 9.78 nm to 15.75 nm at various peaks. The anatase phase is verified by its crystal orientation as shown in figure 1b.

As shown in table 1, crystallite size is measured by Scherrer's equation $D = (0.9\lambda/\beta \cos\theta)$. The dimensionless shape factor K value is closer to unity. The K of about 0.9 typically varies with the actual shape of the crystallite, β - Full Width Half maximum intensity (FWHM), λ - X-ray wavelength represented as Bragg angle Δ (2θ). The TiO_2 of the crystalline anatase phase has a tetragonal structure with lattice parameters "a = b = 3.804 Å" and "c = 9.614 Å" as determined from the JCPDS file 71-1169. The FTIR characterization of the amorphous and anatase TiO_2 showed an absorption spectrum in the range of 400 - 4000 cm^{-1}. The peaks are seen at 400 cm^{-1}, 1724 cm^{-1}, 2922 cm^{-1} and 3410 cm^{-1} that corresponds to vibration of the Ti-O bond, C-O bond, C-H group, and OH stretching, respectively. The band gap energy of 4.01 eV is calculated using the formula $E = hc/\lambda$ with a cut-off wavelength at 489 nm.

Figure 2a illustrates the TEM images of the amorphous phase for the synthesized TiO_2, up to a sintering temperature

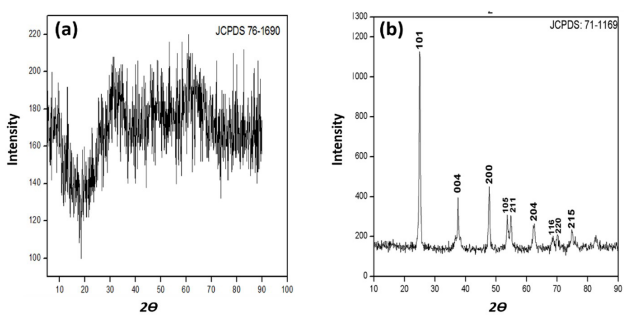

Figure 1: XRD pattern of **(a)** Amorphous TiO_2 and **(b)** Anatase TiO_2.

Table 1: Calculation of crystalline size using Debye-Scherrer for anatase and amorphous TiO_2.

Amorphous phase			Anatase phase		
2θ (Degree)	FWHM (β)	Particle size D (nm)	2θ (Degree)	FWHM (ß)	Crystallite size D (nm)
30.6	3.7	2.14	37.52	0.5042	15.75
34.5	2	3.97	47.74	0.5331	14.9
61.12	1.65	4.82	53.67	0.595	13.35
25.6	1.8	4.41	54.8	0.5805	13.68
63.99	1.1833	4.33	62.35	0.8123	9.78
45.95	1.5	5.29	74.83	0.5567	14.28

of 450 °C. Also, it shows the particles are non-uniformly distributed and with agglomeration. Figure 2b and 2c presents the SEM images of the anatase phase of the synthesized TiO_2 sample submitted to sintering temperature from 450 °C to 750 °C with a particle size of 80 nm to 130 nm showing that the grain boundary size of the crystal has grown thereby removing the holes and defects in the surface of TiO_2.

The grain boundary size increases and the holes and defects disappear making the atoms and molecules get closer to each other. The dielectric constant of the sample stabilizes and reaches a constant value. Figure 3a to 3f shows the Cole-Cole or Nyquist plot containing real and imaginary parts of impedances, an equivalent circuit with resistance and capacitance connected in parallel can be interpreted.

Using Z-plot software, the graphs are fitted to have an equivalent circuit of constant phase elements in parallel with a resistor. The values obtained from the accurate data at 750 °C are presented as: The equivalent circuit consists of Rs = 1.201 KΩ, R1 = 3.050 x 10^6 Ω, CPEIT = 1.201 x 10^{-11} F, CPEIP = 0.984 with the threshold frequency f = 3 x 10^5 Hz where ωτ =1. The dielectric loss and capacitance values at this frequency showed CP = 6.31 x 10^{-11} F. The same calculations are done for all the temperatures 20 °C to 750 °C [19] at an interval of 100 °C. The dielectric constant of TiO_2 is calculated using the equation $C = \epsilon_0 \epsilon_r A/d$, where ϵ_0: Permittivity of vacuum (6.16 x 10^{-11}), ϵ_r: permittivity of TiO_2, A: Area of the pellet (0.785 x 10^{-4}), d: diameter of the pellet (1.7 mm). The procedure to obtain the dielectric constant from Impedance spectroscopy is shown in our earlier work as well [38]. The dielectric constant of the synthesized sample is found to be 88 [38] with a peak frequency of 3 x 10^5 Hz. The observation results in a decrease in the dielectric constant with a rise in frequency. Electronic polarization can orient itself on par with an electric field at a lower frequency rather than at a higher frequency range. With

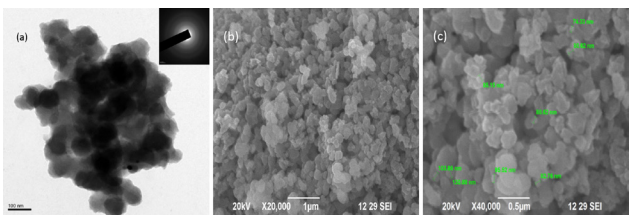

Figure 2: (a) TEM image of amorphous TiO_2 and **(b-c)** SEM image of anatase TiO_2 at magnification of 20,000x and 40,000x.

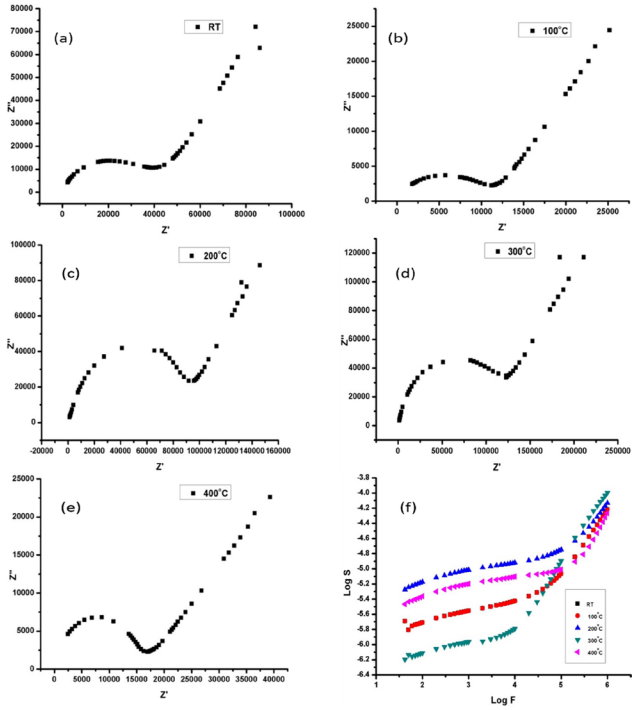

Figure 3: (a-e) Cole-Cole plot and **(f)** Log F vs Log S of synthesized TiO_2 at different temperatures.

an increase in frequency, the capacitance value decreases and then reaches a constant value. The overall dielectric constant of the sample stabilizes at 88 [39].

Conclusion

In this experimental work, TiO_2 nanoparticles are synthesized using sol-gel method. The synthesized TiO_2 was seen in the amorphous phase at a sintering temperature of less than 450 °C whereas the anatase phase was seen at a sintering temperature above 450 °C with the size of crystals ranging from 9.78 nm to 15.75 nm and the size particles varying from 80 nm to 130 nm. The TiO_2 nanocrystals remained in a stable anatase phase when sintered above 450 °C. Titania at nanoscales had an impedance profile with an 88 [39] dielectric constant. When compared with other metal oxides, TiO_2 provides stable electrical properties on par with other metal oxides which makes it feasible to use in creating high-k multi-gate MOSFETs by improving electrical characteristics. However, it has a limitation due to the small band gap. To preserve the interface quality, a layer made of SiO_2/TiO_2 can be used to substitute the current dielectric material SiO_2.

Acknowledgements

The authors would like to thank Karunya University for providing the research lab facilities.

Conflict of Interest

None.

References

1. Sadiq SA, Waseem Z, Hanif S, Riaz S, Hayat K, et al. 2020. Investigation of the role of pH on structural and morphological properties

of titanium dioxide nanoparticles. *IOP Conf Ser Mater Sci Eng* 863(1): 012046. https://doi.org/10.1088/1757-899X/863/1/012046

2. Dubey RS, Krishnamurthy KV, Singh S. 2019. Experimental studies of TiO_2 nanoparticles synthesized by sol-gel and solvothermal routes for DSSCs application. *Results Phys* 14: 102390. https://doi.org/10.1016/j.rinp.2019.102390
3. Maiti CK, Samanta SK, Dalapati GK, Nandi SK, Chatterjee S. 2004. Electrical characterization of TiO_2 gate oxides on strained-Si. *Microelectron Eng* 72(1-4): 253-256. https://doi.org/10.1016/j.mee.2003.12.046
4. Sassi Z, Chafik K, Bureau JC, El Hajbi A. 2002. Surface model of formation of silicon nitride on monocrystalline silicon. *Appl Surf Sci* 187(1-2): 3-17. https://doi.org/10.1016/S0169-4332(01)00436-6
5. Campbell SA, Kim HS, Gilmer DC, He B, Ma T, et al. 1999. Titanium dioxide (TiO_2)-based gate insulators. *IBM J Res Dev* 43(3): 383-392. https://doi.org/10.1147/rd.433.0383
6. Wilk GD, Wallace RM, Anthony J. 2001. High-κ gate dielectrics: current status and materials properties considerations. *J Appl Phys* 89(10): 5243-5275. https://doi.org/10.1063/1.1361065
7. Busani T, Devine RA. 2005. Dielectric and infrared properties of TiO_2 films containing anatase and rutile. *Semicond Sci Technol* 20(8): 870. https://doi.org/10.1088/0268-1242/20/8/043
8. Fukuda H, Namioka S, Miura M, Ishikawa Y, Yoshino M, et al. 1999. Structural and electrical properties of crystalline TiO_2 thin films formed by metalorganic decomposition. *Jpn J Appl Phys* 38(10R): 6034. https://doi.org/10.1143/JJAP.38.6034
9. Gottlob HD, Lemme MC, Mollenhauer T, Wahlbrink T, Efavi JK, et al. 2005. Introduction of crystalline high-k gate dielectrics in a CMOS process. *J Non Cryst Solids* 351(21-23): 1885-1889. https://doi.org/10.1016/j.jnoncrysol.2005.04.032
10. Eriguchi K, Harada Y, Niwa M. 2001. Effects of base layer thickness on reliability of CVD Si_3N_4 stack gate dielectrics. *Microelectron Reliab* 41(4): 587-595. https://doi.org/10.1016/S0026-2714(00)00247-X
11. Chen SM, Ip SY. 1999. Nitrogen in ultra-thin gate oxides: its profile and functions. *Solid State Electron Lett* 43(11): 1997-2003. https://doi.org/10.1016/S0038-1101(99)00166-5
12. Lucovsky G. 1999. Silicon oxide/silicon nitride dual-layer films: a stacked gate dielectric for the 21st century. *J Non Cryst Solids* 254(1-3): 26-37. https://doi.org/10.1016/S0022-3093(99)00432-9
13. Karami A. 2010. Synthesis of TiO_2 nano powder by the sol-gel method and its use as a photocatalyst. *J Iran Chem Soc* 7 (Suppl 2): S154-S160. https://doi.org/10.1007/BF03246194
14. Su C, Hong BY, Tseng CM. 2004. Sol-gel preparation and photocatalysis of titanium dioxide. *Catal Today* 96(3): 119-126. https://doi.org/10.1016/j.cattod.2004.06.132
15. Carp O, Huisman CL, Reller A. 2004. Photoinduced reactivity of titanium dioxide. *Prog Solid State Chem* 32(1-2): 33-177. https://doi.org/10.1016/j.progsolidstchem.2004.08.001
16. Peng B, Jungmann G, Jäger C, Haarer D, Schmidt HW, et al. 2004. Systematic investigation of the role of compact TiO_2 layer in solid state dye-sensitized TiO_2 solar cells. *Coord Chem Rev* 248(13-14): 1479-1489. https://doi.org/10.1016/j.ccr.2004.02.008
17. Sauvage FD, Di Fonzo F, Li Bassi A, Casari CS, Russo V, et al. 2010. Hierarchical TiO_2 photoanode for dye-sensitized solar cells. *Nano Lett* 10(7): 2562-2567. https://doi.org/10.1021/nl101198b
18. Thapa AK, Ishihara T, Moriyama N, Kawamura T, Nakamura H, et al. 2008. Graphite/TiO_2 electrochemical capacitor as a safe electric energy storage system. *ECS Trans* 16(1): 177. https://doi.org/10.1149/1.2985641
19. Phonthammachai N, Chairassameewong T, Gulari E, Jamieson AM, Wongkasemjit S. 2003. Structural and rheological aspect of mesoporous nanocrystalline TiO_2 synthesized via sol-gel process. *Microporous Mesoporous Mater* 66(2-3): 261-271. https://doi.org/10.1016/j.micromeso.2003.09.017
20. Galkina OL, Vinogradov VV, Agafonov AV, Vinogradov AV. 2011. Surfactant-assisted sol-gel synthesis of TiO_2 with uniform particle size distribution. *Int J Inorg Chem* 2011: 108087. https://doi.org/10.1155/2011/108087
21. Zhu Y, Zhang L, Gao C, Cao L. 2000. The synthesis of nanosized TiO_2 powder using a sol-gel method with $TiCl_4$ as a precursor. *J Mater Sci* 35: 4049-4054. https://doi.org/10.1023/A:1004882120249
22. Hema M, Arasi AY, Tamilselvi P, Anbarasan R. 2013. Titania nanoparticles synthesized by sol-gel technique. *Chem Sci Trans* 2(1): 239-245.
23. Santana-Aranda MA, Morán-Pineda M, Hernández J, Castillo S, Gomez R. 2005. Physical properties of TiO_2 prepared by sol-gel under different pH conditions for photocatalysis. *Superficies y Vacío* 18(1): 46-49.
24. Li J, Wan W, Zhou H, Li J, Xu D. 2011. Hydrothermal synthesis of TiO_2(B) nanowires with ultrahigh surface area and their fast charging and discharging properties in Li-ion batteries. *Chem Commun* 47(12): 3439-3441. https://doi.org/10.1039/C0CC04634E
25. Yu X, Wang H, Liu Y, Zhou X, Li B, et al. 2013. One-step ammonia hydrothermal synthesis of single crystal anatase TiO_2 nanowires for highly efficient dye-sensitized solar cells. *J Mater Chem A* 1(6): 2110-2117. https://doi.org/10.1039/C2TA00494A
26. Kim DS, Kwak SY. 2007. The hydrothermal synthesis of mesoporous TiO_2 with high crystallinity, thermal stability, large surface area, and enhanced photocatalytic activity. *Appl Catal A Gen* 323: 110-118. https://doi.org/10.1016/j.apcata.2007.02.010
27. Sun M. 2012. Anticancer activities of nanoencapsulated quercetin in breast cancer cells. Texas Tech University. (Graduate Thesis)
28. Zhang D, Qi L, Ma J, Cheng H. 2002. Formation of crystalline nanosized titania in reverse micelles at room temperature. *J Mater Chem* 12(12): 3677-3680. https://doi.org/10.1039/B206996B
29. Karuppuchamy S, Nonomura K, Yoshida T, Sugiura T, Minoura H. 2002. Cathodic electrodeposition of oxide semiconductor thin films and their application to dye-sensitized solar cells. *Solid State Ion* 151(1-4): 19-27. https://doi.org/10.1016/S0167-2738(02)00599-4
30. Pradhan SK, Reucroft PJ, Yang F, Dozier A. 2003. Growth of TiO_2 nanorods by metalorganic chemical vapor deposition. *J Cryst Growth* 256(1-2): 83-88. https://doi.org/10.1016/S0022-0248(03)01339-3
31. Albertinetti N, Minden HT. 1996. Granularity in ion-beam-sputtered TiO_2 films. *Appl Opt* 35(28): 5620-5625. https://doi.org/10.1364/AO.35.005620
32. Albertin KF, Valle MA, Pereyra I. 2007. Study of TiO_2 and SiO_2/TiO_2 as gate dielectric materials. *ECS Trans* 4(1): 409. https://doi.org/10.1149/1.2813516
33. Brinker CJ, Scherer GW. 1990. Sol-gel Science: The Physics and Chemistry of Sol-gel Processing. Academic Press.
34. Hench LL, West JK. 1990. The sol-gel process. *Chem Rev* 90(1): 33-72. https://doi.org/10.1021/cr00099a003
35. Klein LC, Garvey GJ. 1980. Kinetics of the sol/gel transition. *J Non Cryst Solids* 38: 45-50. https://doi.org/10.1016/0022-3093(80)90392-0
36. Brinker CJ, Keefer KD, Schaefer DW, Ashley CS. 1982. Sol-gel transition in simple silicates. *J Non Cryst Solids* 48(1): 47-64. https://doi.org/10.1016/0022-3093(82)90245-9
37. Wen T, Gao J, Shen J, Zhou Z. 2001. Preparation and characterization of TiO_2 thin films by the sol-gel process. *J Mater Sci* 36: 5923-5926. https://doi.org/10.1023/A:1012989012840
38. Nesamani I, Prabha VL, Paul A, Nirmal D. 2014. Synthesis and dielectric studies of monoclinic nanosized zirconia. *Adv Condens Matter Phys* 2014: 828492. https://doi.org/10.1155/2014/828492
39. Nesamani I. 2015. Performance enhancement of double gate mosfets in sub micron technology using high K dielectric. Faculty of Information and Communication Engineering, Anna University. (Doctoral Dissertation)